

Electronic Supplementary Information

Squaric acid-stimulated electrocatalytic reaction for sensing biomolecules with cycling signal amplification

Wenqiang Lai, Dianping Tang,* Libing Fu, Xiaohua Que, Junyang Zhuang and Guonan Chen*

*Ministry of Education Key Laboratory of Analysis and Detection for Food Safety, Fujian Provincial
Key Laboratory of Analysis and Detection for Food Safety, Department of Chemistry, Fuzhou
University, Fuzhou 350108, PR China*

E-mails: dianping.tang@fzu.edu.cn (D. Tang) and gnchen@fzu.edu.cn (G. Chen).

Fax: +86 591 2286 6135; Tel.: +86 591 2286 6125.

EXPERIMENTAL SECTION

SI.1. Reagents and apparatus

Mouse monoclonal anti-AFP antibody (clone 1G7; designated as mAb₁) and AFP standards (0, 5.0, 10, 20, 50, 100, and 200 ng mL⁻¹) were purchased from Biocell Biotechnol. Co. Ltd. (Zhengzhou, China). L-ascorbic acid was provided from Dingguo Biotech. Co. Ltd. (Beijing, China). Tris(2-carboxyethyl)phosphine (TCEP) was provided from Tokyo Chemical Industry Co. Ltd. (Tokyo, Japan). Squaric acid was obtained from Aladdin Chemistry Co. Ltd. (Shanghai, China). **Cyclobutaneoctol (CBO) was purchased from Hangzhou Chemfar Ltd. (Zhejiang, China).** *N*-(3-dimethylaminopropyl)-*N'*-ethyl-carbodiimide hydrochloride (EDC), *N*-Hydroxysuccinimide (NHS), *N*-2-hydroxyethylpiperazine-*N'*-(2-ethanesulfonic acid), and ferrocenecarboxylic acid (Fc) were obtained from Sigma-Aldrich (USA). HAuCl₄·4H₂O was purchased from Sinopharm Chem. Re. Co. Ltd. (Shanghai, China). All other reagents were of analytical grade and were used without further purification. Ultrapure water obtained from a Millipore water purification system (≥ 18 MΩ, Milli-Q, Millipore) was used in all runs. In the preparation of phosphate buffer solution (PBS) of pH 7.4: NaCl 8.0 g, Na₂HPO₄ 1.15 g, KH₂PO₄ 0.2 g, KCl 0.2 g, were dissolved in 1000 mL double distilled water.

Electrochemical measurements were carried out with a CHI 630D Electrochemical Workstation (Shanghai CH Instruments Inc., China). UV-vis absorption spectroscopy was recorded with an 1102 UV-vis spectrophotometer (Techcomp, China). Graphene-nanogold hybrid nanostructures were characterized using a Philips XL30E scanning electron microscope (SEM, Philips-FEI, The Netherlands) and Renishaw inVia Raman microscopy (Renishaw, The UK).

SI.2. Preparation of graphite oxide and ferrocene-anti-AFP conjugate

Graphite oxide nanosheets were synthesized using a modification of Hummers and Offeman's method from graphite powders.^{S1} Briefly, 2 g of graphite powder was ground with NaCl to reduce the particle size. After removing the salt, the graphite was added to the concentrated H₂SO₄ (80 mL) and left stirring for 2 h. Afterwards, 10 g of KMnO₄ was added

gradually under stirring and the temperature of the mixture was kept to less than 20 °C. Successively, the mixture was stirred at 35 °C for 2 h. Keeping the temperature less than 50 °C, distilled water (180 mL) was added and then the mixture was stirred at room temperature (RT) for 3 h. The reaction was ended by a final addition of distilled water (450 mL) and H₂O₂ (30%, 20 mL). Consequently, the mixture was repeatedly washed with 1 : 10 HCl aqueous solution, and then distilled water. Exfoliation was carried out by sonicating graphene oxide (2 mg mL⁻¹) dispersion under ambient condition for 4 h. Finally, the resulted sample was centrifuged at 8,000 g for 10 min, and the upper solution was taken for future experiments.

Ferrocene-labeled pAb₂ (designated as Fc-pAb₂) was prepared through a typical carbodiimide coupling,^{S2} as shown in Fig. S1-a. Initially, 2.76 mg of ferrocenecarboxylic acid was dissolved thoroughly in 700 μL of *N*-2-hydroxyethylpiperazine-*N'*-(2-ethanesulfonic acid) buffer (50 mmol L⁻¹, pH 9.3), and the pH was then adjusted to 7.3 with 3 mmol L⁻¹ HCl. 11.0 g of NHS and 15.0 mg of EDC were dissolved in the solution followed with continuous stirring for 45 min at room temperature (RT). Following that, 300 μL of 1.0 mg mL⁻¹ anti-AFP antibody dissolved in 50 mmol L⁻¹ pH 7.3 *N*-2-hydroxyethylpiperazine-*N'*-(2-ethanesulfonic acid) buffer was added drop by drop to the mixture under continuous stirring at 150 rpm, and leaved at RT for 20 h. After completion of the incubation, the conjugates were centrifuged for 10 min at 5,000 rpm to remove the precipitates. Finally, the obtained conjugates were dialyzed in a dialysis bag against 0.1 mol L⁻¹ pH 7.4 PBS at RT for 24 h by changing the buffer every 6 h to remove non-conjugated ferrocenecarboxylic acid. The as-prepared Fc-pAb₂ conjugates were dispersed into 500 μL PBS (0.1 mol L⁻¹, pH 7.4) (conc. 0.5 mg mL⁻¹).

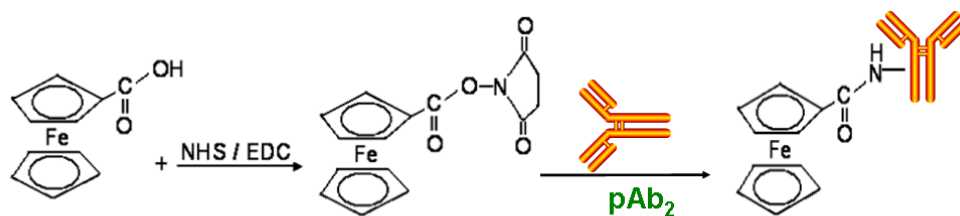


Fig. S1 Fabrication process of Fc-pAb₂

S1.3. Preparation of electrochemical immunosensor

The electrochemical immunosensor was constructed on a cleaned glassy carbon electrode (GCE, 3 mm in diameter) as follows: (i) 5 μL of GO (0.4 mg mL^{-1}) was initially coated on a GCE, and dried for about 30 min (designated as GO/GCE); (ii) electrochemical reduction of Au ions and GO is simultaneously performed at -1.5 V vs. SCE in a solution of 5 mM HAuCl_4 + 10 mM KH_2PO_4 for 500 s (designated as AuNP-GP/GCE);^{S3} (iii) 5 μL of mAb₁ antibody (0.1 mg mL^{-1}) was dropped on the surface of AuNP-GP/GCE, and incubated for 12 h at 4 °C (designated as mAb₁/AuNP-GP/GCE); and (iv) the as-prepared mAb₁/AuNP-GP/GCE, washing with pH 7.4 PBS, was incubated in 2.5 wt% BSA for 60 min at room temperature to eliminate non-specific binding effects and block the remaining active groups. Finally, the obtained electrode (mAb₁/AuNP-GP/GCE) was stored at 4 °C while not in use.

S1.4. Electrochemical measurement

The measurement principle of electrochemical immunosensor is schematically illustrated in [Scheme 1](#). All electrochemical measurements were carried out with a conventional three-electrode system with a modified GCE as working electrode, a platinum foil as auxiliary electrode, and a saturated calomel electrode (SCE) as reference electrode. The detection process was as follows: (i) 5 μL of standards or samples with various concentrations of AFP was dropped to the immunosensor surface, and incubated for 60 min at 37 °C to form the antigen–antibody complex; (ii) after washing with pH 7.4 PBS, 5 μL of Fc-pAb₂ was dropped onto the immunosensor, and incubated for another 60 min at 37 °C to form a sandwiched immunocomplex; and (iii) the obtained electrode was rinsed with water, and differential pulse voltammetry (DPV) measurement from 300 to 700 mV (*vs* SCE) at 50 mV s^{-1} was collected and registered in pH 7.4 PBS solution containing 1.0 mM squaric acid and 1.0 mM TCEP as the signal of the immunosensor relative to AFP concentration. All measurements were conducted at RT ($25 \pm 1.0 \text{ }^\circ\text{C}$). All data were calculated in triplicate.

RESULTS AND DISCUSSION

S2.1. UV-vis characteristics of Fc-pAb₂

Fig. S2 shows UV-vis absorption spectra of various components. Two absorption peaks at

310 and 450 nm were observed for pure ferrocenecarboxylic acid (curve 'a'), while one characteristic peak at 278 nm was obtained for pAb₂ antibody (curve 'b'). When ferrocenecarboxylic acid was labeled onto pAb₂ antibody, however, we only observed one absorption peak at 288 nm (curve 'c'). The peak might be derived from the peak overlapping of ferrocenecarboxylic acid (310 nm) and anti-AFP (278 nm). Importantly, the absorbance of Fc-pAb₂ was obviously lower than those of ferrocenecarboxylic acid and pAb₂ alone.

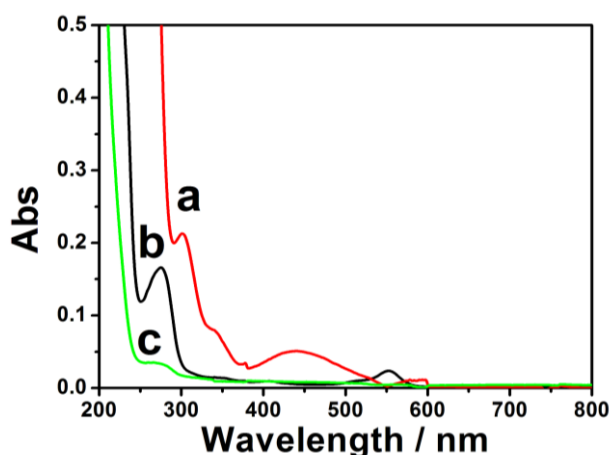


Fig. S2 UV-vis absorption spectra of (a) ferrocenecarboxylic acid, (b) pAb₂, and (c) Fc-pAb₂.

S2.2. Electrochemical characteristics of variously modified electrodes

To monitor the modification process of the immunosensors, electrochemical impedance spectroscopy (EIS) was employed to monitor the interface properties of the electrode after each step. Fig. S3A shows the EIS of variously modified electrodes in 10 mM Fe(CN)₆^{3-/4-} containing 0.1 M KCl. As seen from curve 'b', a relatively large resistance ($R_{ct} \approx 150 \Omega$) was observed at bare GCE. When graphene oxide were coated on the GCE, the resistance greatly increased (curve 'c'), indicating that graphene oxide hindered electron transfer. In contrast, after the formation of AuNP-GP on the GCE, the resistance gently decreased, and seemed a straight line (curve 'a'). This is most likely as a consequence of the fact that AuNP-GP favor for electron transfer between the solution and the electrode. To further clarify this point, AuNPs was directly electrodeposited on the GCE. As seen from curve 'a' in Fig. S3B, small peaks of cyclic voltammogram were observed at graphene oxide-modified GCE, which indicated that the rate of electron transfer was low. When AuNPs was electrodeposited on the

GCE, the peak greatly increased (curve 'b' in Fig. S3B), while the peak of the simultaneous electrodeposited AuNP-GP became higher (curve 'c' in Fig. S3B). Hence, we might make a conclusion that the AuNP-GP could be modified on the GCE by electrochemically deposited method.

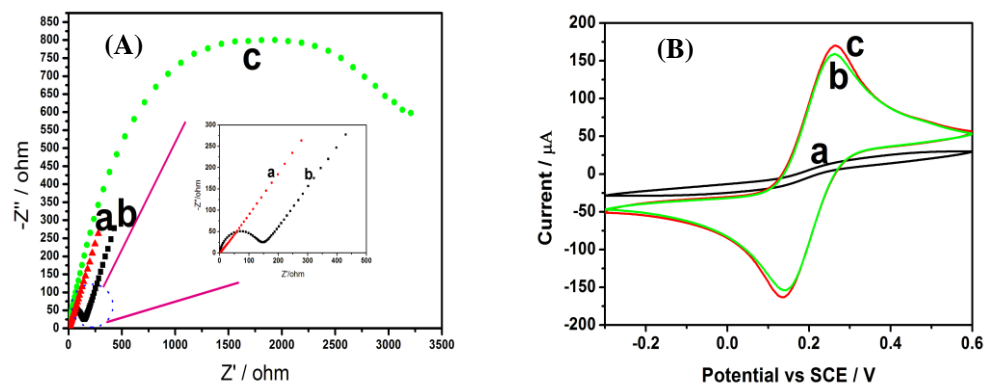


Fig. S3 (A) Electrochemical impedance spectroscopy of (a) AuNP-GP/GCE, (b) GCE, and (c) graphene oxide-modified GCE. (B) Cyclic voltammograms of (a) graphene oxide-modified GCE, (b) AuNP/GCE, and (c) AuNP-GP/GCE in pH 7.4 PBS containing 5 mM $[\text{Fe}(\text{CN})_6]^{3-/4-}$ and 0.1 M KCl. Scan rate: 100 mV s^{-1} .

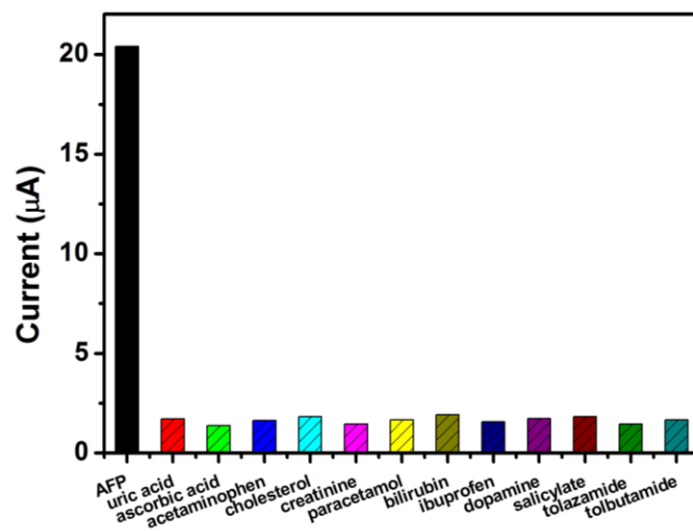


Fig. S4 The specificity of the electrochemical immunoassay (0.1 ng mL^{-1} AFP and 1.0 mM interfering agents used in this case).

Table S1 Comparison of analytical properties of the developed electrochemical immunoassay with other AFP detection methods.

AFP detection method	Linear range	LOD	Ref.
Multiplex electrochemiluminescence immunoassay	0.001 – 0.1 pg mL ⁻¹	0.4 fg mL ⁻¹	S4
Chemiluminescence imaging	0.001 – 100 ng mL ⁻¹	0.27 pg mL ⁻¹	S5
Multiplex amperometric immunoassay	0.016 – 50 ng mL ⁻¹	5.4 pg mL ⁻¹	S6
Fluorescence image immunoassay	10 – 800 ng mL ⁻¹	3.9 ng mL ⁻¹	S7
Label-free electrochemical immunoassay	0.1 – 100 ng mL ⁻¹	60 pg mL ⁻¹	S8
Sandwich-type electrochemical immunoassay	0.06 – 200 ng mL ⁻¹	1.7 pg mL ⁻¹	S9
Simultaneous electrochemical immunoassay	0.5 – 200 ng mL ⁻¹	7.8 pg mL ⁻¹	S10
Near-infrared electrochemiluminescence immunoassay	0.01 – 80 ng mL ⁻¹	5.0 pg mL ⁻¹	S11
Photoelectrochemical immunoassay	0.0005 – 10 µg mL ⁻¹	0.13 pg mL ⁻¹	S12
Reagentless amperometric immunoassay	0.05 – 200 ng mL ⁻¹	20 pg mL ⁻¹	S13
Near-infrared luminescent immunoassay	0.5 – 18 ng mL ⁻¹	200 pg mL ⁻¹	S14
Reflectometric interference spectroscopy	-	100 ng mL ⁻¹	S15
SERS-based immunoassay	0 -10 ng mL ⁻¹	-	S16
Surface plasmon resonance immunoassay	1.0 – 200 ng mL ⁻¹	650 pg mL ⁻¹	S17
Microcantilever-based immunoassay	0.1 – 100 ng mL ⁻¹	-	S18
Systematic evolution of ligands by exponential enrichment	12.5 – 800 ng mL ⁻¹	-	S19
Fluorescence polarization immunoassay	0.5 – 500 ng mL ⁻¹	280 pg mL ⁻¹	S20
SQA-based electrochemical immunoassay	0.001 – 200 ng mL ⁻¹	0.6 pg mL ⁻¹	This work

Table S2 Comparison of the assayed results for clinical serum specimens by using the electrochemical immunosensor and the referenced ECL method.

Sample no.	Method; Concentration (mean \pm SD, $n = 3$, ng mL ⁻¹)		t_{exp}
	Found by the immunosensor	Found by the ECL	
1	1.0 \pm 0.1	1.1 \pm 0.1	1.22
2	4.7 \pm 0.4	4.5 \pm 0.2	0.77
3	7.4 \pm 0.9	6.6 \pm 0.6	1.28
4	58.1 \pm 5.4	50.3 \pm 3.0	2.18
5	7.5 \pm 0.8	7.9 \pm 0.7	0.65
6	78.3 \pm 3.4	81.6 \pm 3.6	1.15
7	126.2 \pm 8.0	133.4 \pm 5.8	1.26
8	3.5 \pm 0.2	3.3 \pm 0.2	1.22
9	9.1 \pm 0.8	9.8 \pm 0.8	1.07
10	38.6 \pm 4.1	35.1 \pm 2.3	1.29
11	18.2 \pm 1.2	20.3 \pm 0.7	2.62
12	27.8 \pm 0.9	25.6 \pm 1.1	2.68
13	65.9 \pm 3.4	62.3 \pm 2.4	1.49
14	145.6 \pm 4.2	154.3 \pm 3.5	2.76
15	123.3 \pm 5.6	112.9 \pm 4.3	2.55
16	87.4 \pm 2.1	90.3 \pm 3.2	1.31
17	92.1 \pm 4.3	89.7 \pm 3.9	0.72

Notes and references

- S1. W. Hummers and R. Offeman, *J. Am. Chem. Soc.*, 1958, **80**, 1339.
- S2. V. Kandimalla, V. Tripathi and H. Ju, *Biomaterial*, 2006, **27**, 1167.
- S3. Y. Zhou, J. Chen, F. Wang, Z. Sheng and X. Xia, *Chem. Commun.*, 2010, **46**, 5951.
- S4. Z. Guo, T. Hao, S. Du, B. Chen, Z. Wang, X. Li and S. Wang, *Biosens. Bioelectron.*, 2013, **44**, 101.
- S5. C. Zong, J. Wu, J. Xu, H. Ju and F. Yan, *Biosens. Bioelectron.*, 2013, **43**, 372.
- S6. Q. Zhu, Y. Chai, R. Yuan, Y. Zhuo, J. Han, Y. Li and N. Liao, *Biosens. Bioelectron.*, 2013, **43**, 440.
- S7. X. Yu, H. Xia, Z. Su, Y. Lin, K. Wang, J. Yu, H. Tang, D. Pang and Z. Zhang, *Biosens. Bioelectron.*, 2013, **41**, 129.
- S8. L. Lin, Z. Wei, H. Zhang and M. Shao, *Biosens. Bioelectron.*, 2013, **41**, 342.
- S9. Q. Zhu, R. Yuan, Y. Chai, J. Han, Y. Li and N. Liao, *Analyst*, 2013, **138**, 620.
- S10. F. Kong, B. Xu, J. Xu and H. Chen, *Biosens. Bioelectron.*, 2013, **39**, 177.
- S11. G. Liang, S. Liu, G. Zou and X. Zhang, *Anal. Chem.*, 2012, **84**, 10645.
- S12. Y. Li, M. Ma and J. Zhu, *Anal. Chem.*, 2012, **84**, 10492.
- S13. X. Huang, X. Deng and D. Wu, *Anal. Methods*, 2012, **4**, 3575.
- S14. Q. Wei, Y. Lei, W. Xu, J. Xie and G. Chen, *Dalton Transactions*, 2012, **41**, 11219.
- S15. Y. Kurihara, M. Takama, T. Sekiya, Y. Yoshihara, T. Ooya and T. Takeuchi, *Langmuir*, 2012, **28**, 13609.
- S16. M. Lee, K. Lee, K. Kim, K. Oh and J. Choo, *Lab Chip*, 2012, **12**, 3720.
- S17. R. Liang, G. Yao, L. Fan and J. Qiu, *Anal. Chim. Acta*, 2012, **737**, 22.
- S18. D. Lee, D. Kwon, W. Ko, J. Joo, H. Seo, S. Lee and S. Jeon, *Chem. Commun.*, 2012, **48**, 7182.
- S19. C. Huang, H. Lin, S. Shiesh and G. Lee, *Biosens. Bioelectron.*, 2012, **35**, 50.
- S20. J. Tian, L. Zhou, Y. Zhao, Y. Wang, Y. Peng and S. Zhao, *Talanta*, 2012, **92**, 72.